Electronic Supplementary Material (ESI) for ChemComm.

Electronic supplementary information for

A new metal-organic framework constructed from both cationic node and cationic linker for highly efficient anion exchange

Mi Zhou,[a,b] Zhanfeng Ju[a] and Daqiang Yuan*[a]

[a] *State Key Laboratory of Structural Chemistry, Fujian Institute of Research on the Structure of Matter, Chinese Academy of Sciences, Fujian, Fuzhou, 350002, China*

[b] *University of Chinese Academy of Sciences, Beijing 100049, People's Republic of China*

Table of contents

Materials and Instrumentation

Methyl 4-hydroxybenzoate, hexamethylenetetramine, cyclohexane diamine, $In(NO_3)_3·xH_2O$, $Cu(NO_3)_2·6H_2O$, trifluoroacetic acid (TFA), acetonitrile (CH_3CN) and *N*,*N*-dimethylformamide (DMF) were commercially available and used as received. ^1H NMR spectra were recorded on a Bruker Avance 400 spectrometer (400.1 MHz for ^1H NMR). Powder X-ray diffraction (PXRD) data were collected on a Rigaku MiniFlex 600 diffractometer working with Cu Kα radiation, and the recording speed was 3° min^{-1} over the 2θ range of 4−50° at room temperature. Crystal structure data were collected on a SuperNova diffractometer equipped with a copper micro-focus X-ray sources (λ = 1.54184 Å) and an Atlas CCD detector or a Bruker APEX-III CCD diffractometer with graphite-monochromated Cu Kα radiation (λ = 1.54178 Å). UV-Vis absorption spectra were recorded in a quartz cuvette with a Lambda 365 spectrophotometer. Fourier transform infrared (FT-IR) spectra of the samples were recorded on KBr pellets in the 400−4000 cm^{-1} range using a VERTEX70 spectrometer. Elemental analyses (C, H, N) were performed on an Elementar Vario MICRO elemental analyzer. Thermogravimetric analyses (TGA) were recorded on a NETZSCH STA 449C unit at a heating rate of 10 ^oC min^{-1} under a nitrogen atmosphere.

Synthesis of $H_2L^{2+}(NO_3)_2$

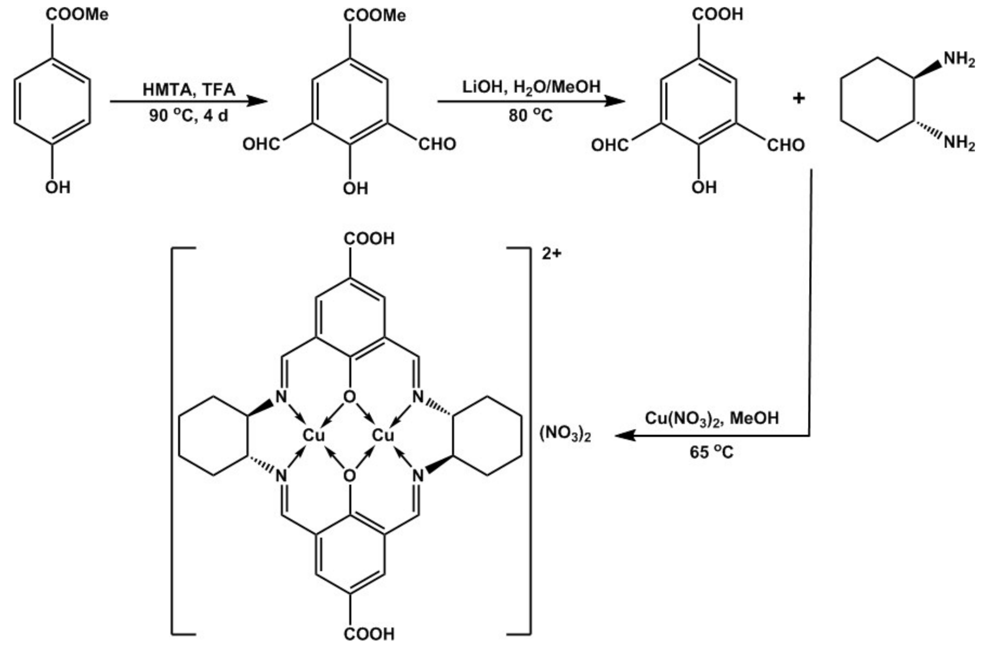

Scheme S1 the synthetic route of $H_2L^{2+}(NO_3)_2$

Methyl 3,5-diformyl-4-hydroxybenzoate was synthesized according to the literature[1, 2]. Methyl 4-hydroxybenzoate (6.8 g, 44.3 mmol) and hexamethylenetetramine (25.58 g, 182.5 mmol) were dissolved in 50 mL TFA and the solution was heated at 90 ^{o}C for 4 d. Then 300 mL H_2O was added to the solution and the mixture was heated up to give a homogeneous solution. After cooling, yellow needle-like product crystallized out, dried in vacuum, about 6.5 g, yield (70%). ^{1}H NMR (400 MHz, $CDCl_3$) δ 12.07 (s, 1H), 10.30 (s, 2H), 8.67 (s, 2H), 3.98 (s, 3H).

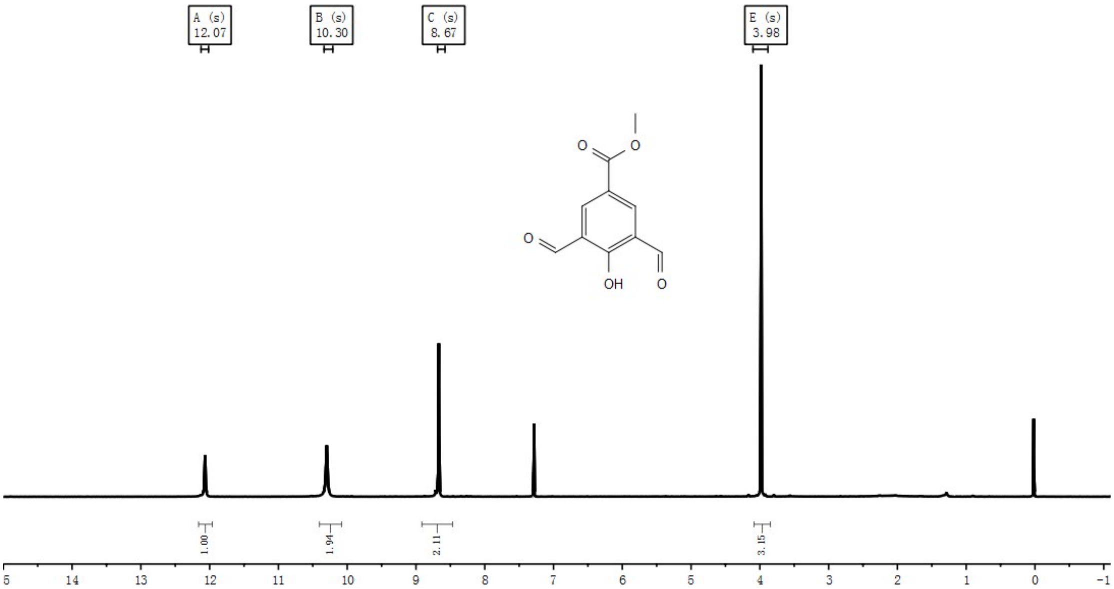

Figure S1 ^{1}H NMR spectra of 3,5-diformyl-4-hydroxybenzoate

3,5-diformyl-4-hydroxybenzoic acid: 200 mL H_2O and 50 mL methanol was charged into a 500 mL bottle containing 2.08 g ester and 2 g LiOH, the mixture was heated at 80 ^{o}C overnight. Then the yellow solution was evaporated most of the methanol by rotary evaporation, aqueous HCl solution was added subsequently to adjusted the pH to 2 and the precipitate was filtered out and dried at vacuum, about 1.85 g, yield (95%). ^{1}H NMR (400 MHz, DMSO) *δ* 10.28 (s, 2H), 8.52 (s, 2H).

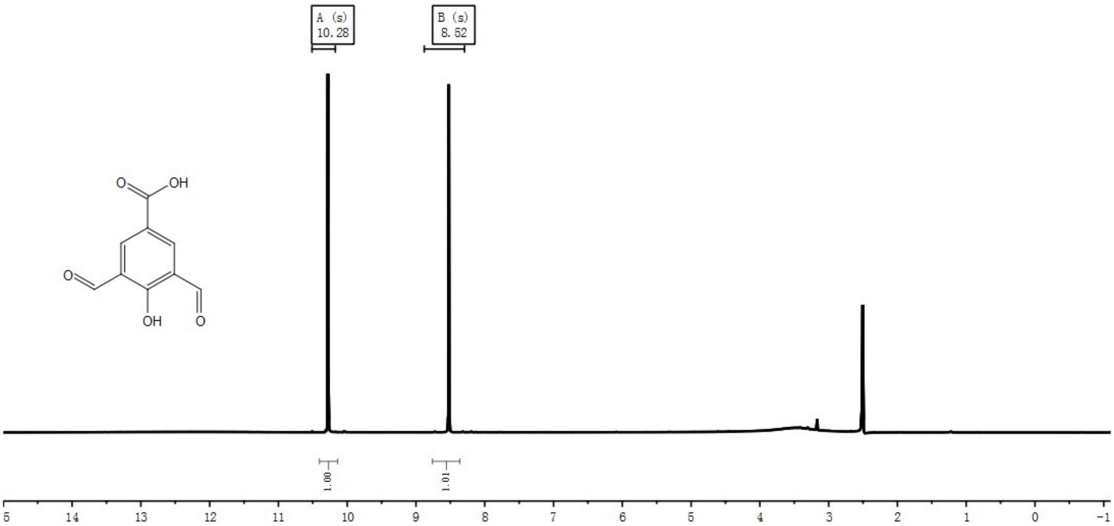

Figure S2 ^{1}H NMR spectra of 3,5-diformyl-4-hydroxybenzoic acid

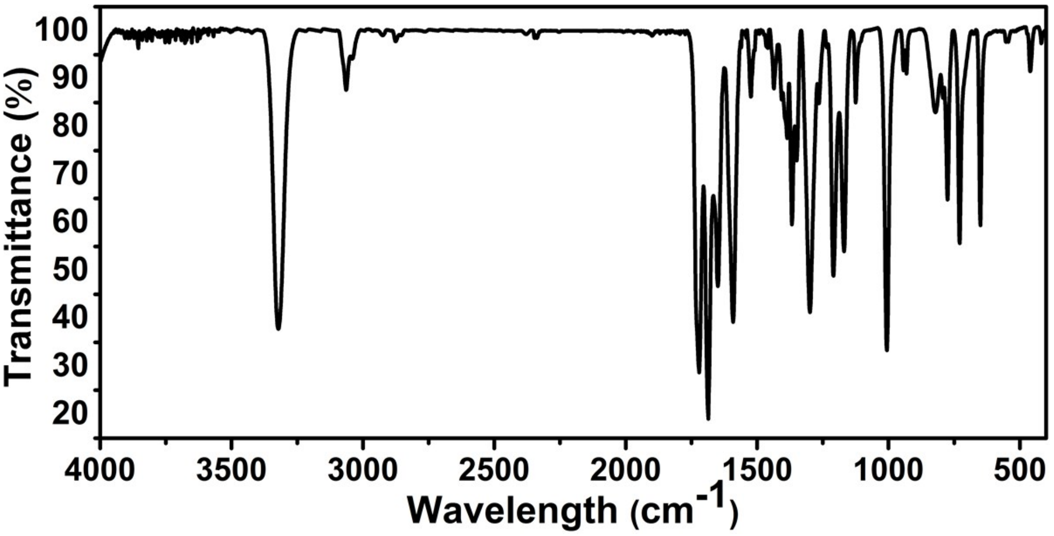

Figure S3 IR spectrum of 3,5-diformyl-4-hydroxybenzoic acid. The peak at 3323 cm^{-1} indicates the presence of phenolic hydroxyl. Peak near 3071 cm^{-1} corresponds to the O-H of carboxylic acid. The peaks at 1723 cm^{-1}, 1693 cm^{-1} and 648 cm^{-1} indicate the presence of aldehyde group.

$H_2L^{2+}(NO_3)_2$: 19.4 mg aldehyde (0.1 mmol) dissolved in 3 mL ethanol with heat, the mixture of 38 mg $Cu(NO_3)_2 \cdot 6H_2O$ (1.3 equiv.) and 11.4 mg (1*R*,2*R*)-cyclohexane diamine (1 equiv.) in 2 mL ethanol was added, heated in a sealed vial at 65 ^oC without stir for 7 d, black needle-like crystal appeared, about 35 mg, yield (60%). The racemic ligand was synthesized with similar method except the (1*R*,2*R*)-cyclohexane diamine was replaced by racemic one.

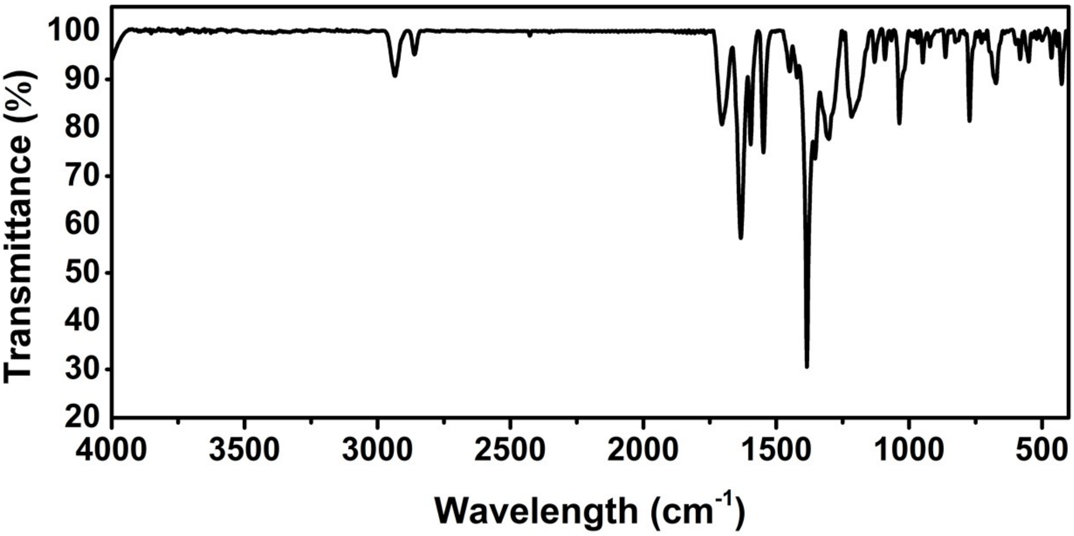

Figure S4 IR spectrum of $H_2L^{2+}(NO_3)_2$. The peaks near 2937 cm^{-1} and 2855 cm^{-1} correspond to the C-H of cyclohexane. The peak of 1708 cm^{-1} indicates the presence of C=O of carboxylic acid. The peak near 1636 cm^{-1} corresponds to the C=N. The peak near 1380 cm^{-1} indicates the presence of NO_3^-. The peak near 427 cm^{-1} corresponds to the Cu-O in the ligand.

Synthesis of FJI-Y6

5 mg ligand and 15 mg $In(NO_3)_3$ was added to a 10 mL vial contain 1 mL DMF and 1 mL CH_3CN, then 20 μL HBF_4 was added into the mixture, the vial was sealed and placed in an 80 ^oC oven for 3 d, black prism crystals of **FJI-Y6** was harvested by decanted the solution, yield (40%) according to the ligand. Elemental analysis for $C_{180}H_{180}N_{24}O_{44}Cu_{12}In_6 \cdot 14NO_3^- \cdot 34H_2O$: calc.(%): C: 34.24 H: 3.96 N: 8.43; found(%): C: 34.29 H: 4.07 N: 8.32. *rac*-**FJI-Y6** was synthesized with similar method except racemic ligand was employed. **FJI-Y6⊃dye** was harvested by immersing **FJI-Y6** in 10 mL DMF contain 17.5 mg (50 μmol) AO7 for 2 d.

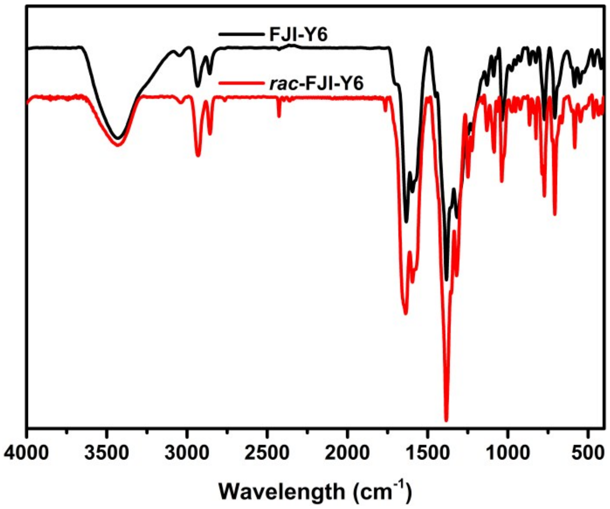

Figure S5 FT-IR spectrum of FJI-Y6, *rac*-FJI-Y6: the broad peak at 3429 cm^{-1} corresponds to the O-H of H_2O. Peaks near 2940 cm^{-1} and 2858 cm^{-1} correspond to the C-H of cyclohexane in the ligand. The peak near 1639 cm^{-1} corresponds to the C=N of the ligand. The peak near 1382 cm^{-1} indicates the presence of NO_3^-.

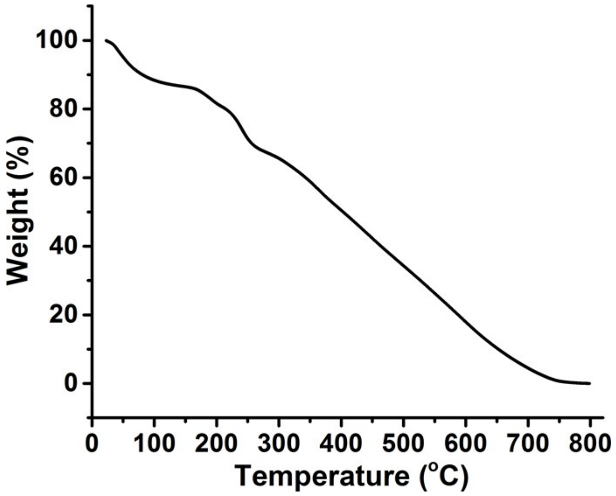

Figure S6 TG curve of FJI-Y6

Single-crystal X-ray data

Single-crystal X-ray data of $H_2L^{2+}(NO_3)_2$, *rac*-$H_2L^{2+}(NO_3)_2$, **FJI-Y6** and *rac*-**FJI-Y6** were collected on a SuperNova, Dual, Cu at zero, Atlas diffractometer. Single-crystal X-ray data of **FJI-Y6⊃**dye were collected at 290 K using graphite-monochromated Cu Kα radiation (λ=1.54178Å) on a Bruker APEX-III CCD diffractometer. The crystals of $H_2L^{2+}(NO_3)_2$, *rac*-$H_2L^{2+}(NO_3)_2$ and **FJI-Y6** were directly put on the diffractometer and the data were collected under 100 K, 100 K and 200 K, respectively; *rac*-**FJI-Y6** and **FJI-Y6⊃**dye were sealed in silica tube with mother liquid and were kept at 293 K and 290 K during data collection, respectively. The structures were solved by direct methods and refined by full-matrix least-squares on F^2 with anisotropic displacement using the *SHELXTL*-2016 software package[3] The non-H atoms were treated anisotropically, whereas the aromatic and hydroxy- and alkyl-hydrogen atoms were placed in calculated, ideal positions and refined as riding on their respective carbon atoms. Free solvent molecules were highly disordered, and attempts to locate and refine the solvent peaks were unsuccessful. The diffused electron densities resulting from these residual solvent molecules were removed from the dataset using the SQUEEZE routine of PLATON and refined further using the data generated.[4] The contents of the solvent region are not represented in the unit cell contents in the crystal data. The details for data collection and refinement are included in the CIF file in the Supporting Information. The crystal structure refinement data were listed in Table S1. CCDC Number: 1586541, 1586542, 1822395-1822397.

Table S1. Crystal data and structure refinement for $H_2L^{2+}(NO_3)_2$, *rac*-$H_2L^{2+}(NO_3)_2$, FJI-Y6, *rac*-FJI-Y6 and FJI-Y6⊃dye

Identification code	$H_2L^{2+}(NO_3)_2$	*rac*-$H_2L^{2+}(NO_3)_2$	FJI-Y6	*rac*-FJI-Y6	FJI-Y6⊃dye
CCDC No.	1586542	1822397	1586541	1822396	1822395
Empirical formula	$C_{32}H_{46}Cu_2N_6O_{14}$	$C_{32}H_{38}Cu_2N_6O_{14}$	$C_{15}H_{14}CuIn_{0.50}N_3O_{6.67}$	$C_{15}H_{14}CuIn_{0.50}N_3O_{6.67}$	$C_{90}H_{84}Cu_6In_3N_{12}O_{22}$
Formula weight	865.83	857.76	463.91	463.91	2411.39
T (K)	100.0(2)	99.9(5)	200.0(1)	293.0(2)	290.0(2)
λ (Å)	1.54184	1.54184	1.54184 Å	1.54184 Å	1.54178 Å
Crystal system	Monoclinic	monoclinic	hexagonal	hexagonal	trigonal
Space group	$P2_1$	$P2_1$/c	$P6_3$/mmc	$P6_3$/mmc	P-3_1c
a (Å)	8.73490(10)	8.70380(10)	21.8599(3)	22.8847(5)	23.0639(3)
b (Å)	13.3687(2)	13.4115(2)	21.8599(3)	22.8847(5)	23.0639(3)
c (Å)	15.7886(2)	15.6432(2)	30.9566(2)	30.1026(6)	30.1054(3)
α (°)	90	90	90	90	90
β (°)	104.319(2)	103.055(2)	90	90	90
γ (°)	90	90	120	120	120
V	1786.42(4)	1778.85(4)	12810.9(4)	13652.9(7)	13868.8(4)
Z	2	2	12	12	2
D_{calc} (g/cm^3)	1.610	1.601	0.722	0.677	0.577
μ (mm^{-1})	2.143	2.151	2.986	2.801	2.664
F(000)	900	884	2782	2782	2410
Reflections collected	6857	6962	50173	31829	101698
Independent reflections	4913 [R(int) = 0.0238]	3480 (Rint = 0.0178)	4674 [R_{int} = 0.0653]	4987 (Rint = 0.1001)	9058 (Rint = 0.0526)
Goodness-of-fit on F^2	1.037	1.046	1.052	1.037	1.040
Final R indices [I>2σ(I)]	$R1$ = 0.0401, $wR2$ = 0.1089	$R1$ = 0.0342, $wR2$ = 0.0838	$R1$ = 0.0758, $wR2$ = 0.2052	$R1$ = 0.0604, $wR2$ = 0.1780	$R1$ = 0.0597, $wR2$ = 0.1815
R indices (all data)	$R1$ = 0.0408, $wR2$ = 0.1095	$R1$ = 0.0383, $wR2$ = 0.0862	$R1$ = 0.1016, $wR2$ = 0.2486	$R1$ = 0.0712, $wR2$ = 0.1948	$R1$ = 0.0693, $wR2$ = 0.1957
Absolute structure parameter	0.00(3)	-	-	-	-

Dyes adsorption and release experiment

Dye adsorption by FJI-Y6

6 mL 8.33×10^{-5} mol·L^{-1} DMF solution of dye was charged into a vial containing 10 mg **FJI-Y6**, then the UV-Vis absorbance measurements were performed periodically for the upper clear solution, which was poured back to the original system after each measurement to keep the total amount of sample constant. The absorbance at maximum wavelength was chosen to calculate the dye content of anion-exchange progress by the formula:

$$C(\mathrm{d})=A_t/A_0\times100\%$$

C(d) is the content of the dye in solution; A_0 is the absorbance of the tested at 0 h; A_t is the absorbance of the tested at the different time in the anion-exchange process.

Dye release experiment

After complete adsorption of AO7, the release experiment was conducted by replacing the upper clear liquid with 6 mL DMF solution containing 170 mg (2 mmol) $NaNO_3$. The recycle experiment of adsorption and release was conducted for 5 cycles. UV-Vis was measured after completion of adsorption and release for each cycle.

Ion-exchange capacity experiment

20 mg (21.6 μmol) MOF was added into 10 mL DMF contain 17.5 mg (50 μmol) AO7 (the molar ratio of NO_3^-:SO_3^- = 1:1). The dye solution was diluted for UV-VIS measurement due to the high concentration of dye in solution. The screwed vial was put on a shaking bed to accelerate the exchange. 100 μL the upper clear liquid was sucked out and diluted by 5.9 mL DMF for UV-Vis measurement. After exchanged for 1 d, about 13.9 μmol AO7 was remained in the solution, about 72.2% NO_3^- was exchanged by AO7. After exchanged for 2 d, about 12.03 μmol AO7 remained in the solution, about 75.9% NO_3^- was exchanged by AO7 (Fig. S22). The crystallinity was also maintained according to the PXRD (Fig. S23).

Abbreviation for those dyes: MLB^+ = Methylene blue, SD I = Sudan I, $AR88^-$= Acid red 88, $AO7^-$ = Acid orange 7, $AB1^{2-}$ = Acid black, OG^{2-} = Orange G, $CS3B^{2-}$ = Crocein scarlet 3B, MB^{2-} = Methyl blue, $Amar^{3-}$ = Amaranth. The dimensions of the dyes are defined as x×y×z (x≤y≤z) according to the literature.[5-7]

Table S2. The dimensions of the dye molecules

Abbr.	MLB	SD I	AR88	AO7	AB1	OG	CS3B	MB	Amar
charge	+1	0	-1	-1	-2	-2	-2	-2	-3
Mw	284.40	248.28	377.39	327.33	570.51	406.38	510.50	753.82	604.47
x(Å)	4.00	3.68	5.44	5.44	5.44	5.44	5.44	13.89	7.72
y(Å)	7.93	9.74	10.27	10.03	11.55	10.14	10.61	14.35	10.45
z(Å)	16.34	13.55	15.66	15.67	22.93	15.64	21.81	24.49	14.34

The molecule structure of dyes utilized as follow:

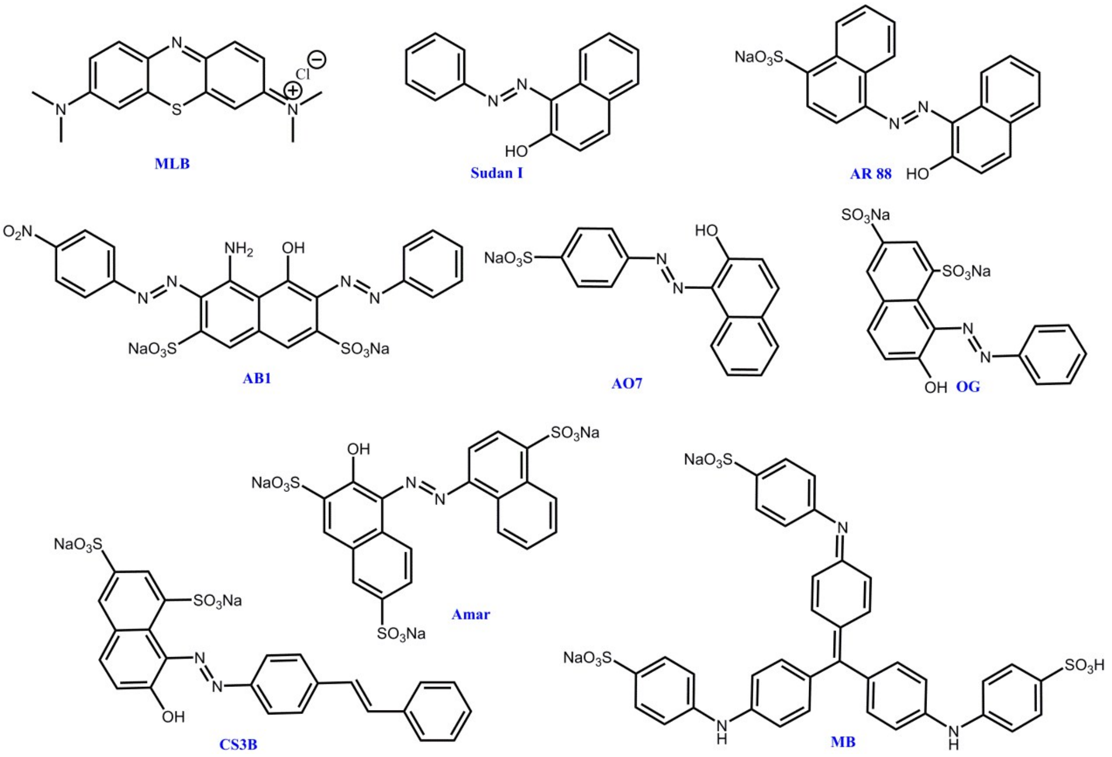

Scheme S2 The molecule structure of dyes.

UV-Vis absorption spectra changes of dyes in presence of FJI-Y6

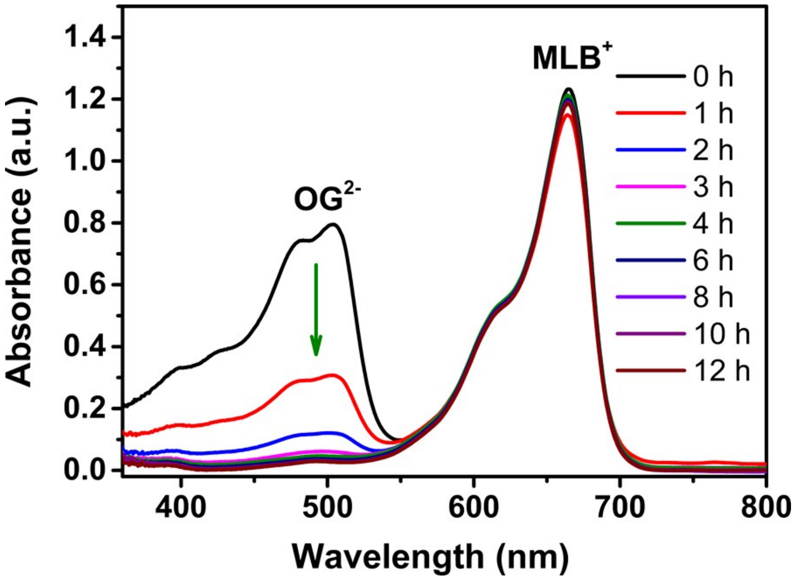

Figure S7 The UV-Vis absorption spectral changes of the mixture solution of OG^{2-} and MLB^{+} in the presence of **FJI-Y6**

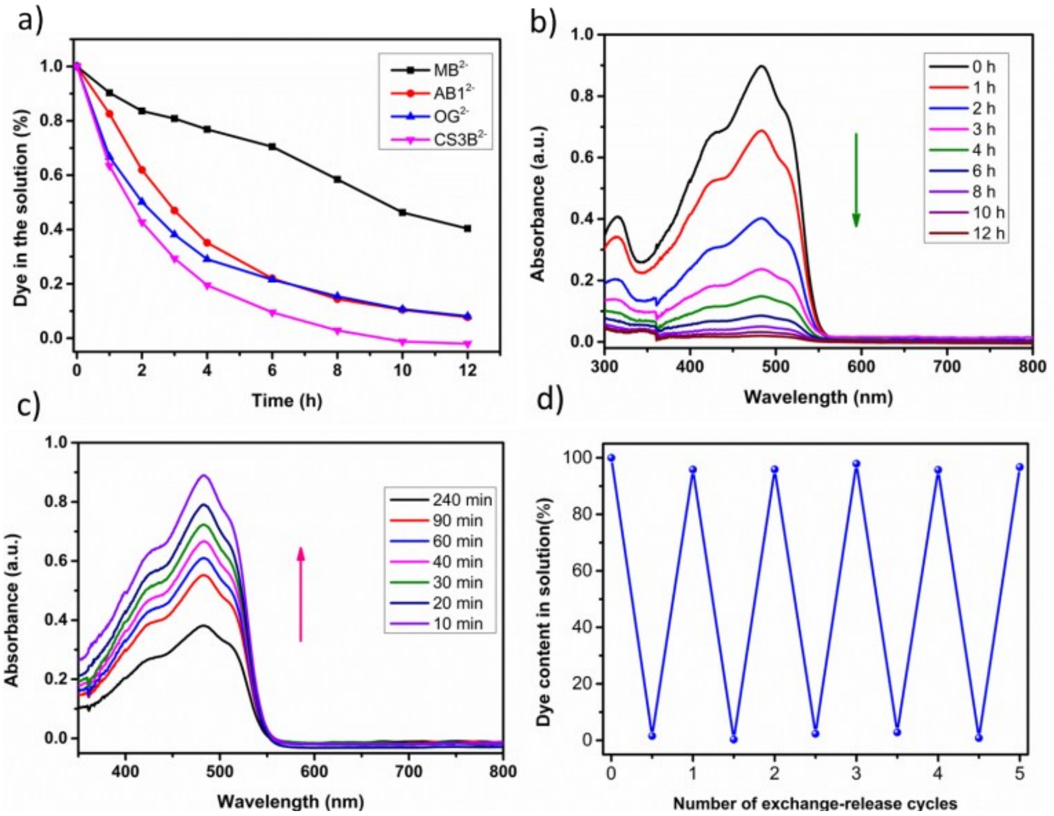

Figure S8 a) The content of anionic dyes in diverse size in the solution monitored with time in the presence of **FJI-Y6**. b) UV-Vis spectra monitored with time during the loading process of $AO7^{-}$ for **FJI-Y6**. c) UV-Vis spectra monitored with time during the release process of $AO7^{-}$ for **FJI-Y6**. d) Number of load-release cycles.

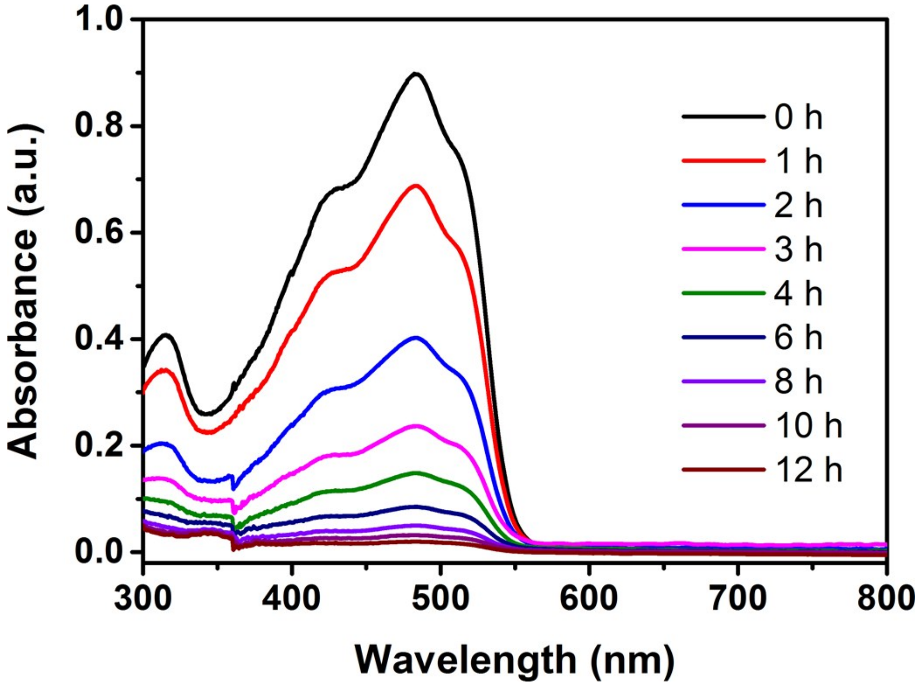

Figure S9 The UV-Vis absorption spectral changes of AO7 in the presence of **FJI-Y6**

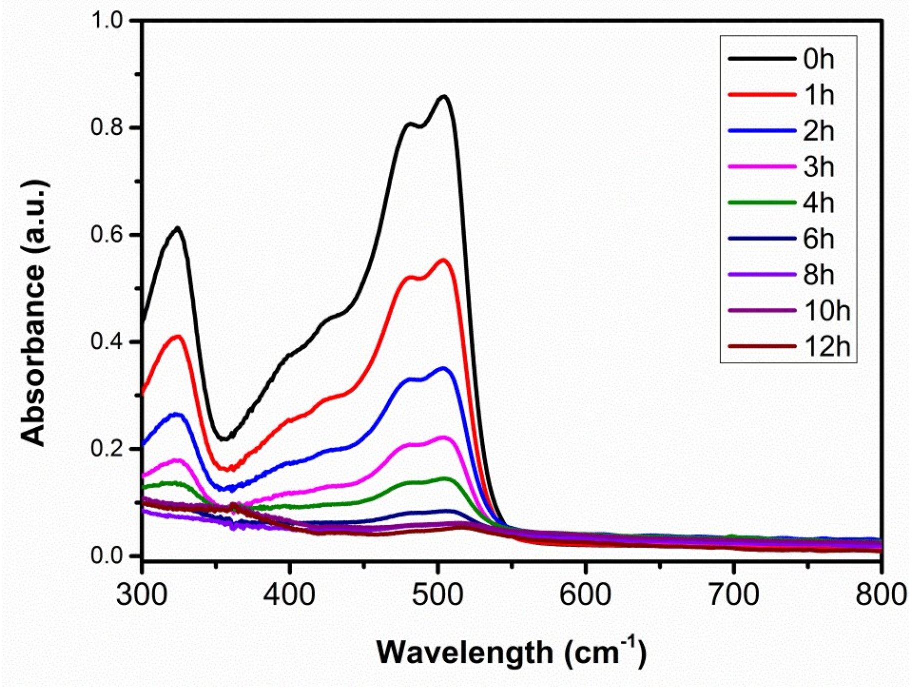

Figure S10 The UV-Vis absorption spectral changes of OG in the presence of **FJI-Y6**

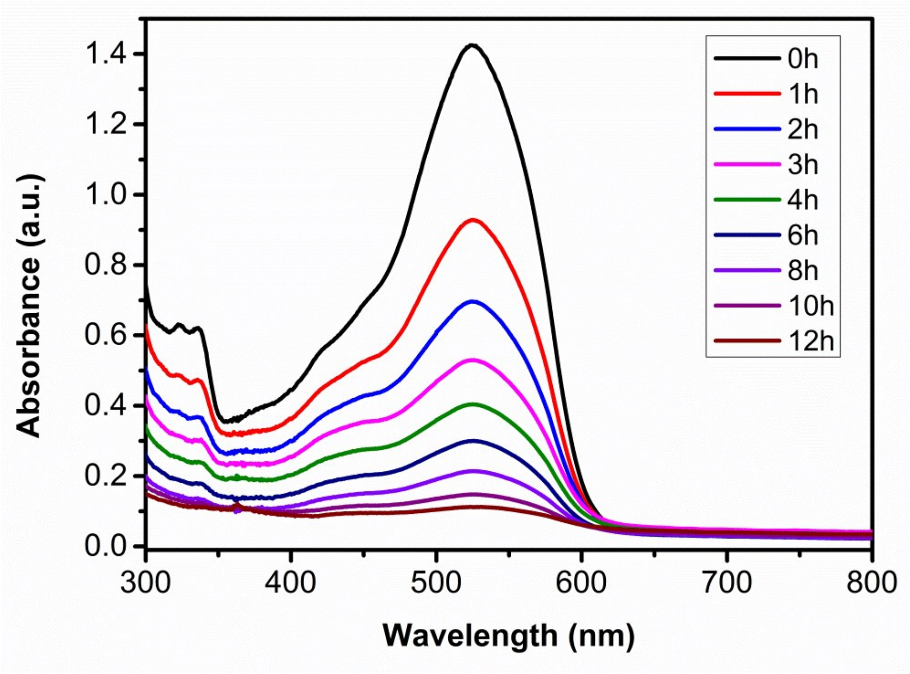

Figure S11 The UV-Vis absorption spectral changes of AMAR in the presence of **FJI-Y6**

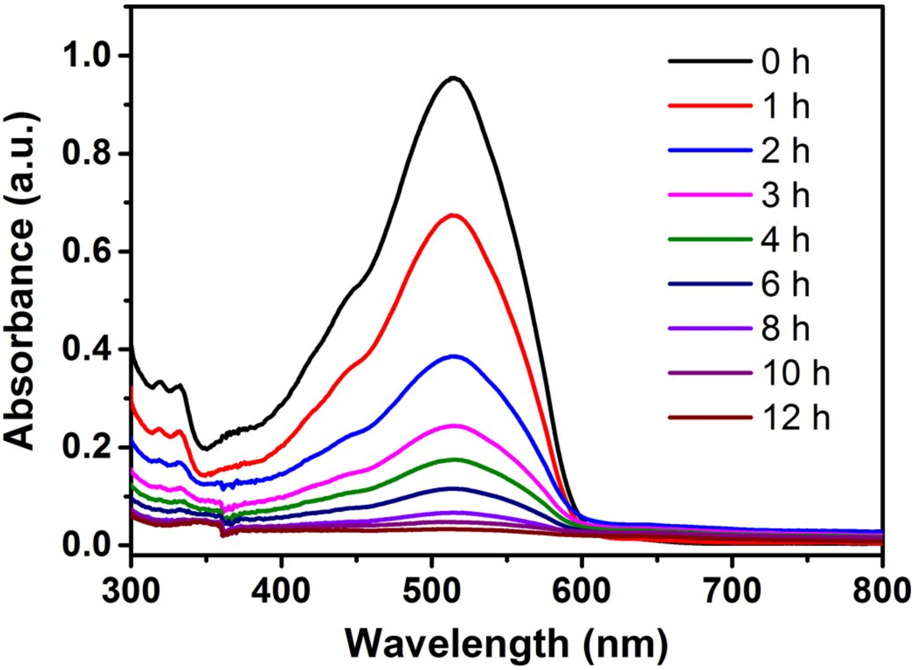

Figure S12 The UV-Vis absorption spectral changes of AR88 in the presence of **FJI-Y6**

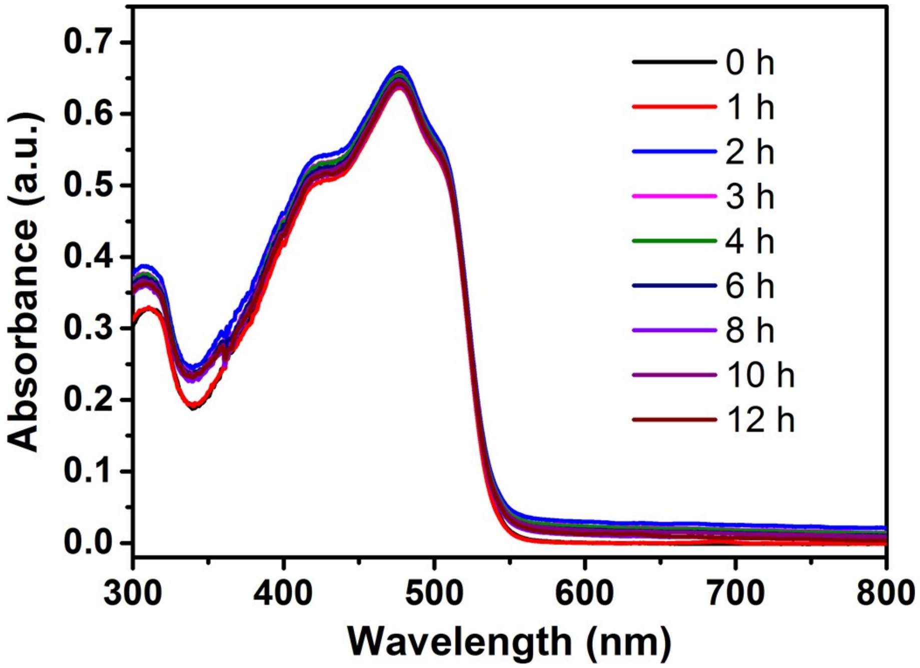

Figure S13 The UV-Vis absorption spectral changes of Sudan I in the presence of **FJI-Y6**

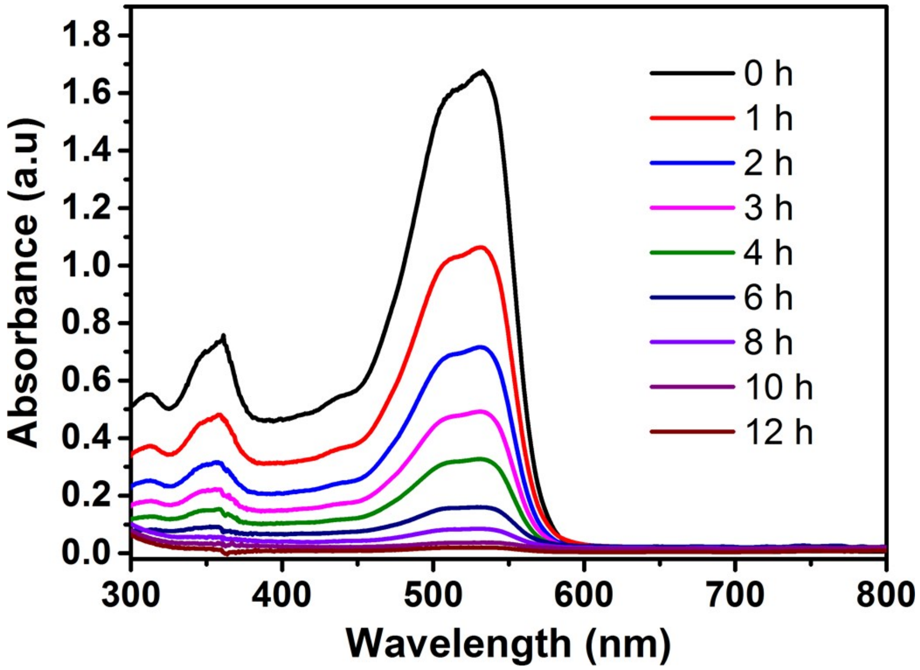

Figure S14 The UV-Vis absorption spectral changes of CS3B in the presence of **FJI-Y6**

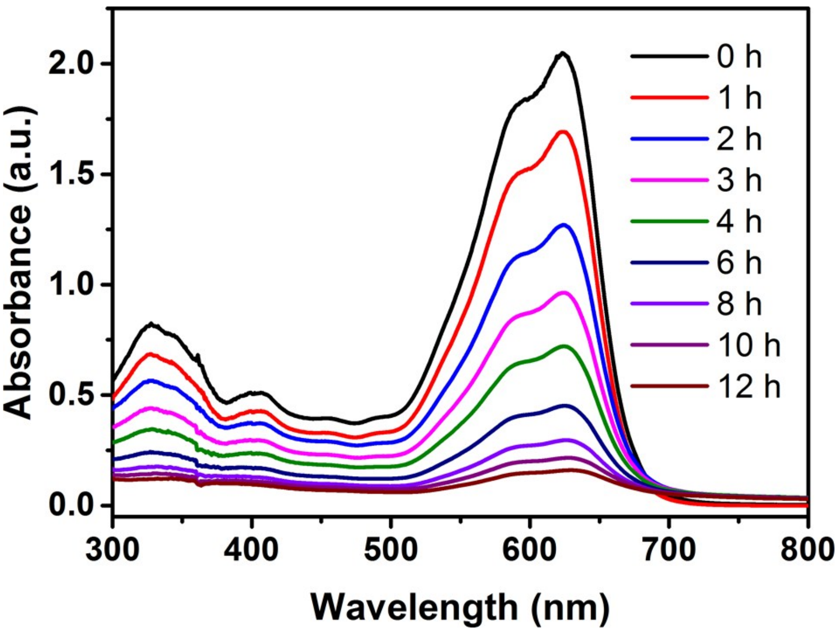

Figure S15 The UV-Vis absorption spectral changes of AB1 in the presence of **FJI-Y6**

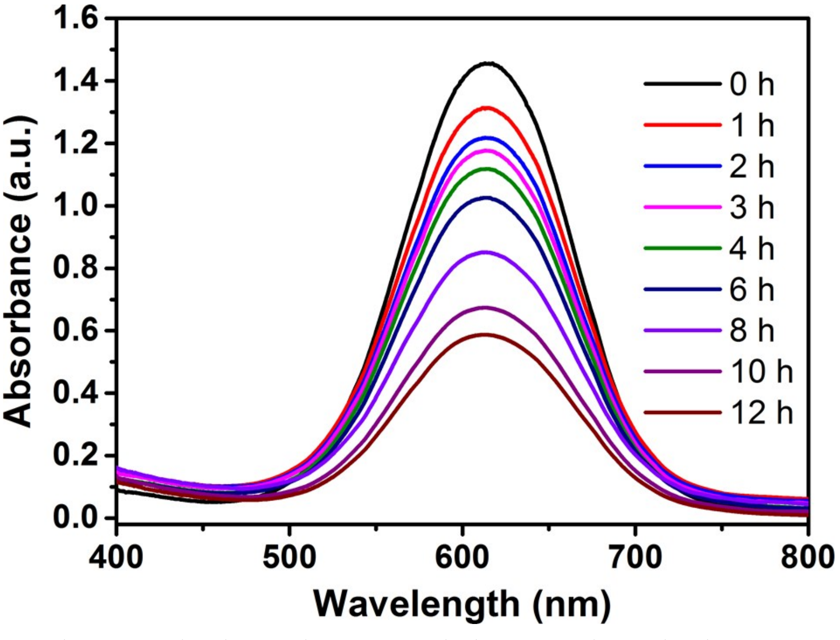

Figure S16 The UV-Vis absorption spectral changes of MB in the presence of **FJI-Y6**

Photo, IR, UV-Vis spectrum and PXRD of FJI-Y6 after dyes adsorption

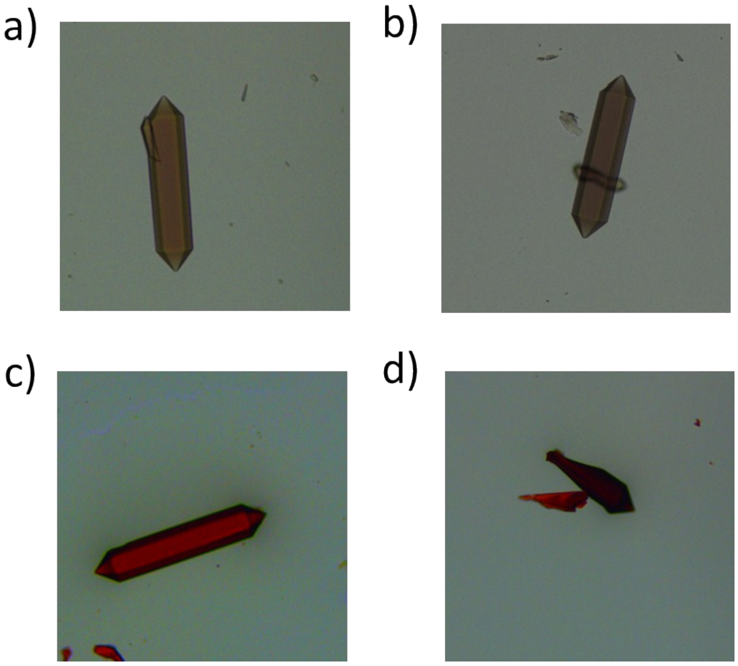

Figure S17 The photographs of FJI-Y6 crystal before and after dye-exchange, the crystal after dye-adsorption was washed with DMF for few times before took a photo under a microscope. a) Fresh sample. b) After exchanged with SDI. c) After exchanged with AO7. d) After exchanged with OG.

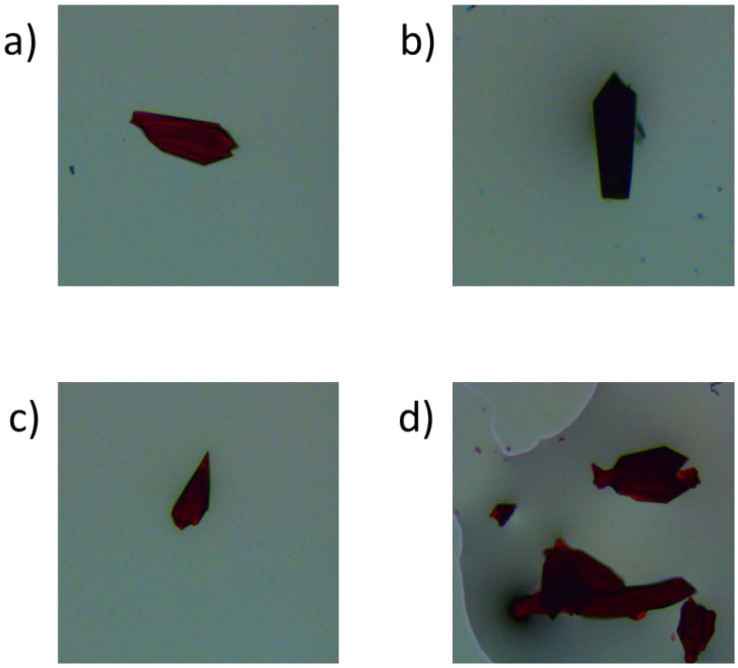

Figure S18 The photographs of FJI-Y6 crystal after dye-exchange, the crystal after dye-adsorption was washed with DMF for few times before took a photo under a microscope. a) After exchanged with AMAR. b) After exchanged AB10B. c) After exchanged with CS3B. d) After exchanged with AR88.

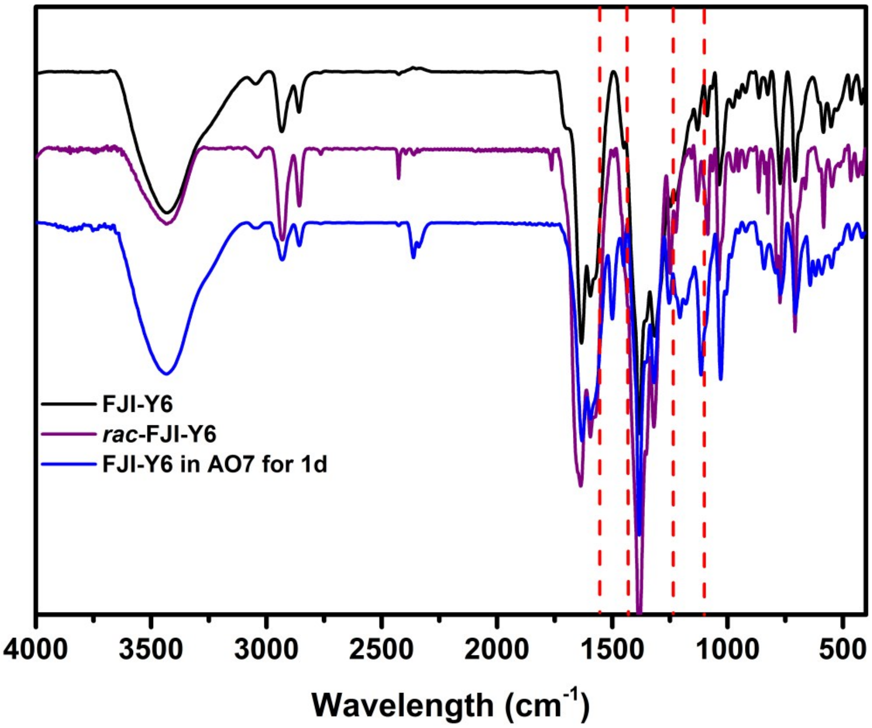

Figure S19 The FT-IR spectrum of FJI-Y6, *rac*-FJI-Y6 and FJI-Y6 after exchanged with AO7$^-$ for 1 d (after washed by DMF for several times) from top to bottom, respectively. The peak around 1490 cm^{-1} corresponds to the N=N group in AO7$^-$. The peak around 1200 cm^{-1} and 1110 cm^{-1} correspond to the –SO$_3^-$ group in AO7$^-$.

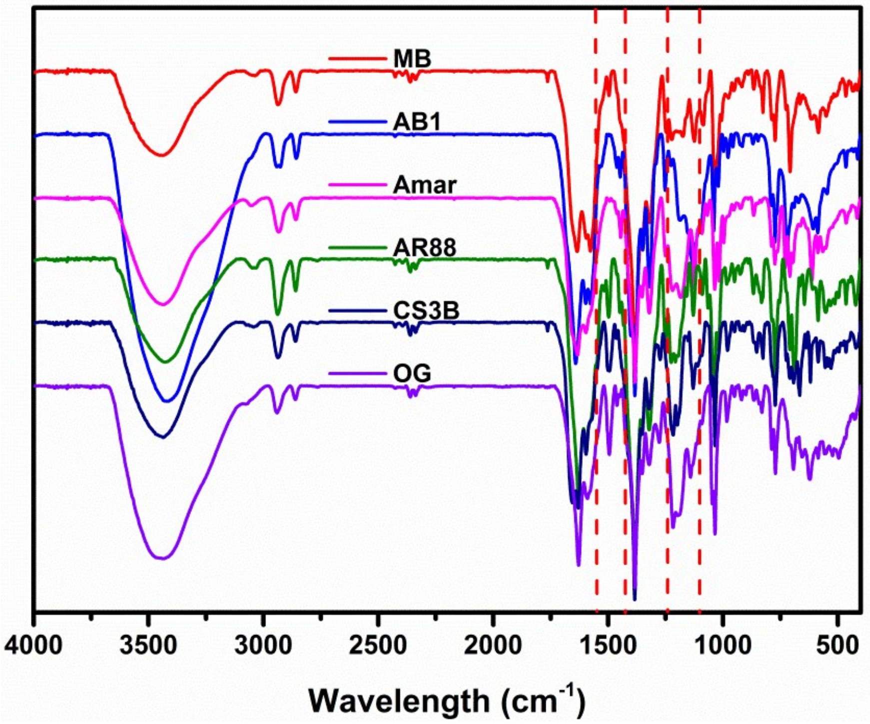

Figure S20 The FT-IR spectrum of FJI-Y6 after exchanged with MB, AB1, Amar, AR88, CS3B and OG for 1 d respectively (after washed by DMF for several times).

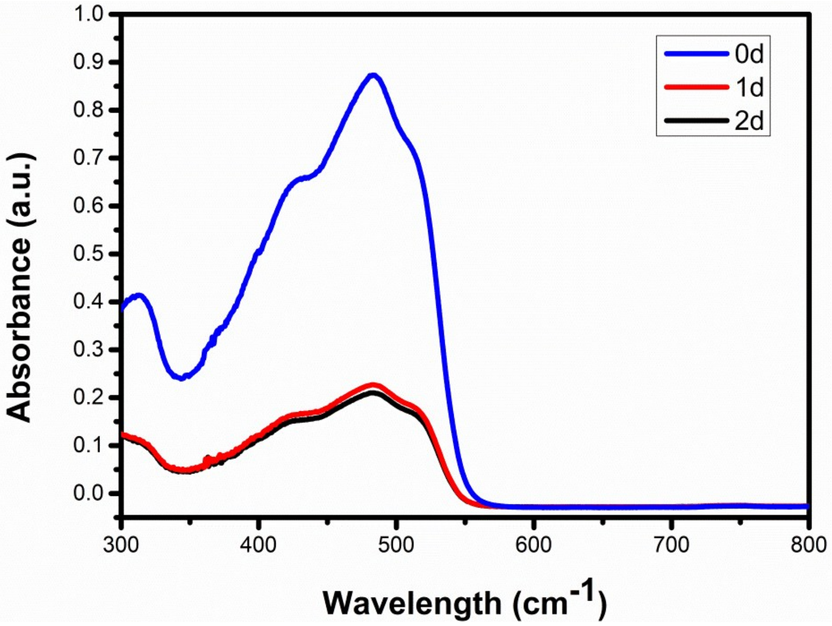

Figure S21 The UV-Vis absorption spectral changes of diluted AO7 solution in the presence of FJI-Y6

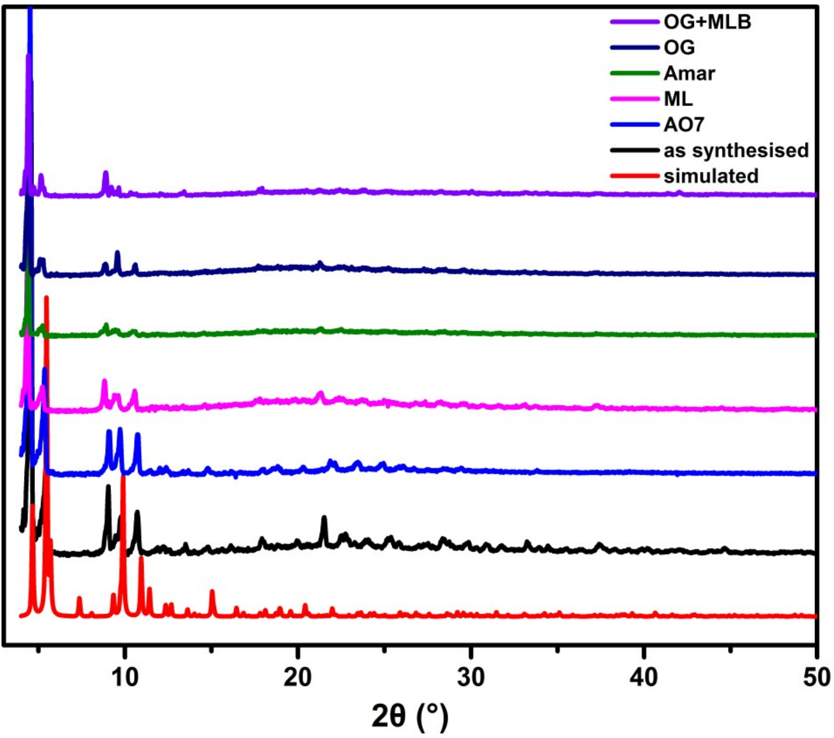

Figure S22 The PXRD of **FJI-Y6** after dyes adsorption

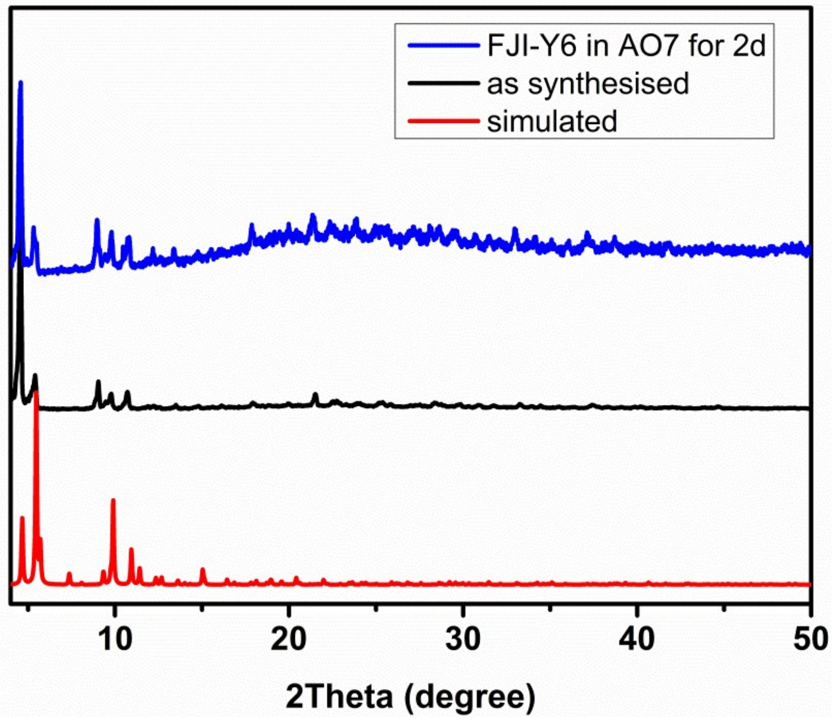

Figure S23 The PXRD of FJI-Y6 after immersed in high concentration AO7 solution for 2 d.

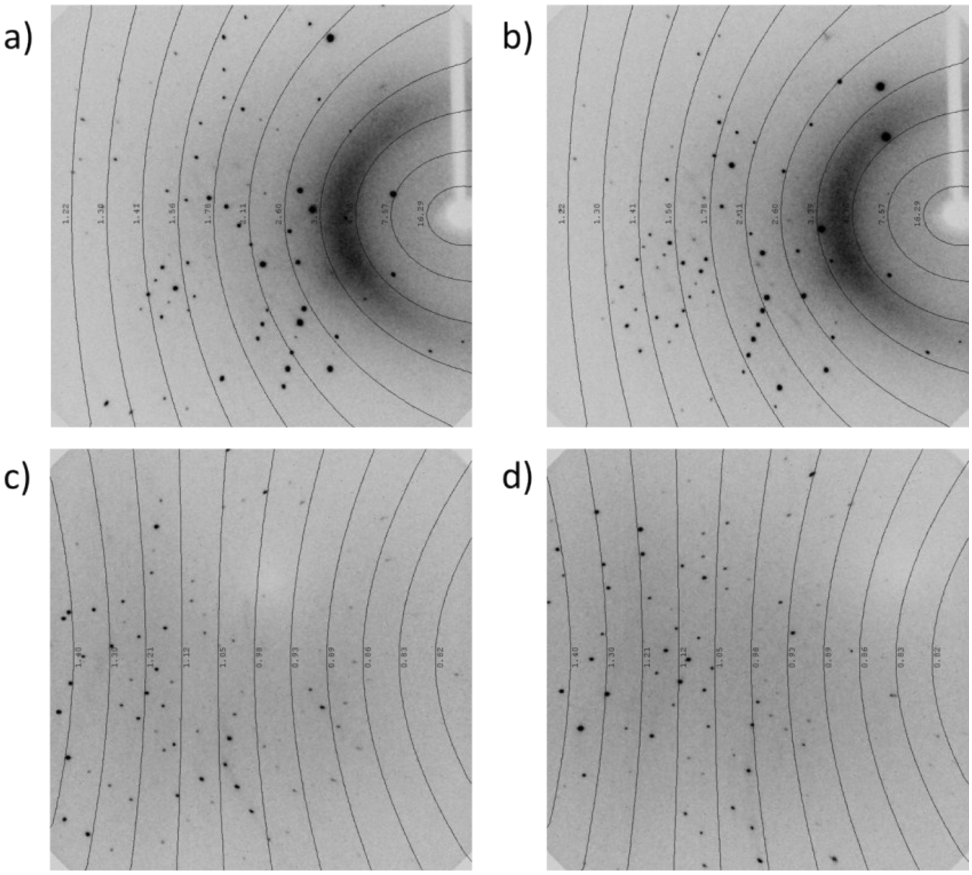

Figure S24 The diffraction frames of FJI-Y6 after loaded AO7

Additional Structure figures

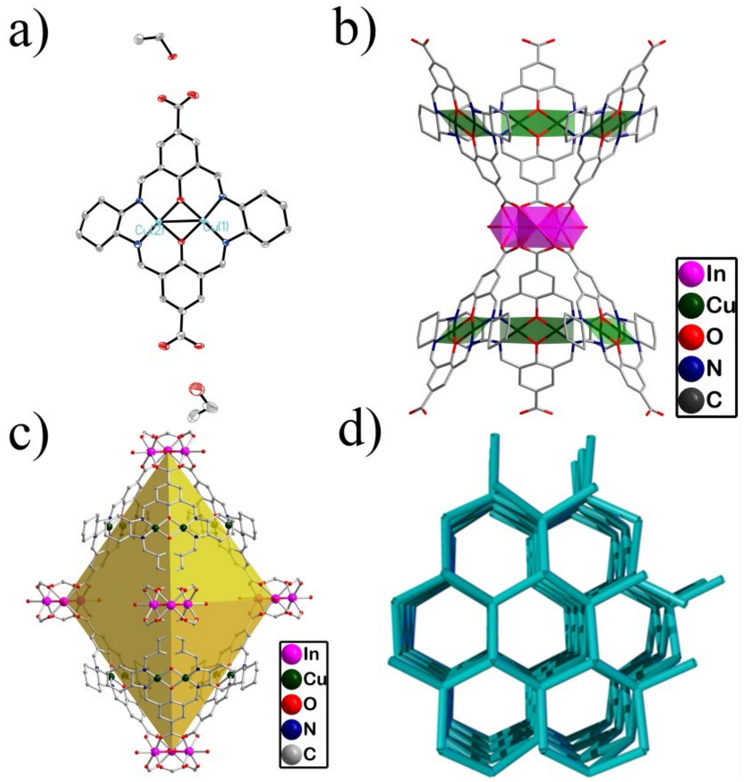

Figure S25 a) The structure of ligand. b) Six ligands coordinate with $In_3O(CO_2)_6(H_2O)_3^+$. c) The trigonal bipyramid cages in FJI-Y6. d) The simplified *acs* topology of FJI-Y6

Reference

1. L. F. Lindoy, G. V. Meehan and N. Svenstrup, *Synthesis*, 1998, 1029-1032.
2. T. Routasalo, J. Helaja, J. Kavakka and A. M. P. Koskinen, *Eur. J. Org. Chem.*, 2008, 3190-3199.
3. G. M. Sheldrick, *Acta Crystallogr. A*, 2008, **64**, 112-122.
4. A. L. Spek, *J. Appl. Crystallogr.*, 2003, **36**, 7-13.
5. X. Zhao, X. Bu, T. Wu, S. T. Zheng, L. Wang and P. Feng, *Nat. Commun.*, 2013, **4**, 2344.
6. B. Q. Song, X. L. Wang, Y. T. Zhang, X. S. Wu, H. S. Liu, K. Z. Shao and Z. M. Su, *Chem. Commun.*, 2015, **51**, 9515-9518.
7. J. A. Johnson, X. Zhang, T. C. Reeson, Y. S. Chen and J. Zhang, *J. Am. Chem. Soc.*, 2014, **136**, 15881-15884.